Theoretical Analysis of Micro-Piezo Motors

Jairaj Jangle [1], Prajwal Langde [2], Siddhesh Girase [3], Abhay Chopde [4]
[1,2,3,4] *Department of Electronics Engineering, Vishwakarma Institute of Technology, Pune 411037*

Abstract- **Piezoelectric motors are recent type of actuators in the field of MEMS (Micro Electro-Mechanical Systems). These motors work on the principle of inverse piezoelectric effect which have many other applications such as in micro sensors, actuators, resonators, filters, hydrophones etc. Functional and different drive techniques categorize these motors into three groups: resonance-drive (piezoelectric ultrasonic motors), inertia-drive, and piezo-walk-drive. In this paper, a brief summary of piezoelectric motors, with their classification, analysis is presented.**

Index Terms- **PZT(Lead Zirconate Titanate (Pb[Zr(x)Ti(1-x)]O3)), Inverse Piezoelectric effect, resonance-drive, piezo shear actuation, stick-slip, slip-slip, miniaturization, standing and travelling wave.**

I. INTRODUCTION

Micro-electromechanical systems (MEMS) are devices of the scale of a few micrometers, which integrate electrical and mechanical elements. The main advantage of using MEMS is that they are economical and show precise motion when subjected to very small electric field. Piezoelectric motors are electro-mechanical actuators, which convert the limited displacement of a piezoceramic material into rotatory or translatory motion of a rotor or a slider. Such motors have wide range of advantages. Absence of friction results in increase of resolution to a few nanometers. They do not require use of any lubricant and thus are ideal for ultra-high vacuum applications. Resolutions of piezo motors range from 1μm to 100μm, applied force capability in orders of thousands of Newtons and works in the wide temperature range of -200°C to 200°C. There is no magnetic field involved in operation of piezo motor and hence is not affected by external factor such as temperature and external magnetic interference, thus can be used in applications like MRI scanning where high magnetic field is involved. Another advantage of non-magnetic drive of piezo micro motors is that their scalability range is high because the force caused by magnets is reduced drastically when scaled down in micrometer range. Acceleration could be of the range of 10,000 g and the response time is in microseconds. One of the biggest advantages of piezo motors is that they exhibit very high holding torque, that is, even if the motor is de-energized, it will still exhibit torque in orders of 10 N-cm. Micro piezo motor find their applications in various fields including high precision length measurement, medical micro robots, actuators in camera lenses for aperture and focal length variation, micro swarm robots and Optical Coherence Tomography (OCT) in dermatology. These are fabricated using methods like those used to construct integrated circuits. Size makes it possible to integrate it into wide range of systems. In inverse piezoelectric effect, a mechanical strain is produced in the material when a potential difference is applied across it. On application of analog voltage signals, piezoelectric materials can show uniform deformation varying with time, which is specially used in case of micro piezo motors. There are various materials, which possess this behaviour such as quartz, bernilite, topaz etc. There is a large variety of drive designs exploiting the motion obtainable from inverse piezoelectric effect. These drives vary on the basis of principle of operation, for e.g. ultrasonic driven, walk type etc. Some of the very common drives have been discussed in the upcoming text.

Upcoming sections II covers Piezo Walk Type Motor, III covers Inertia Drive Motor and IV covers Ultrasonic Piezoelectric motor. Section V winds up with a conclusion and section VI mentions the papers and websites, which helped up, compile this paper.

II. PIEZO-WALK TYPE MOTOR

Mathematical model describing deflection and elongation of piezoelectric bimorph can be derived using basic mechanics principles of static equilibrium and strain compatibility between layers of bimorph. The model is developed on the basis of inverse piezoelectric effect and Euler-Bernoulli theory of elastic deformation. Single leg is considered as cantilever and only the forces generated by inverse piezoelectric effect are included. Results showing relative static deflection and elongation of the leg, driven by voltages V1 and V2 are given by-

$$x = \frac{3}{4}\frac{d_{33}L^2}{tD}(V_1 - V_2) \quad (1)$$

$$y = L\frac{d_{33}}{2t}(V_1 - V_2) \quad (2)$$

In (1) and (2) constant d33 is piezoelectric charge constant, L is the length of leg, D is the half width of the leg, t is the thickness of a single piezoelectric layer.

1. OVERVIEW AND WORKING

Piezo-walk type (piezo stepping drives) usually consists of several individual piezo actuators, which are in contact with the bar which impose a preload on the actuators, and generate motion through a series of coordinated clamping-unclamping and shear motion cycles. With respect to Figure 1, firstly, the preload is imposed on actuators 'A', due to which they form a contact with the ceramic runner. This is referred as clamping action. Meanwhile, the actuators 'B' lose contact with the runner causing unclamping action. A potential is then applied to both A and B so as to produce a shear bending in both of these in opposite direction, which eventually causes linear motion of the runner. When this entire process is repeated with actuators 'B' clamping the runner, a cycle is said to be completed. Each cycle provides only a few microns of movement.

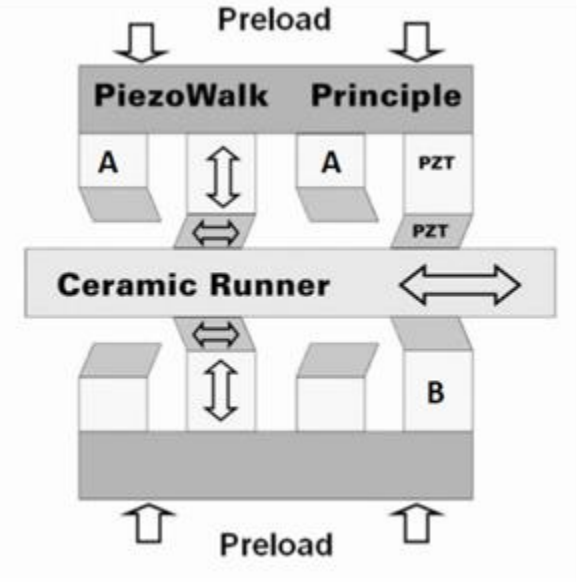

Figure 1: Working principle of piezo walk drive.

When applied for a continuous duration, this drive produces continuous motion in mm/second range. These piezo actuators perform a walking motion (and hence, the name) that causes a forward feed of the runner. The piezo actuators can be used to perform very miniature walking and feed motion so that a high motion resolution of the range of nanometers is achieved.

2. TYPES OF PIEZO-WALK DRIVEN MOTORS

(a) NEXLINE

The most typical kind of piezo-drive motor is Nexline, which works on the principle discussed above. Piezo actuators with high-load walking capacity drive clamping-unclamping and shear movement in order to move the runner in a linear motion.

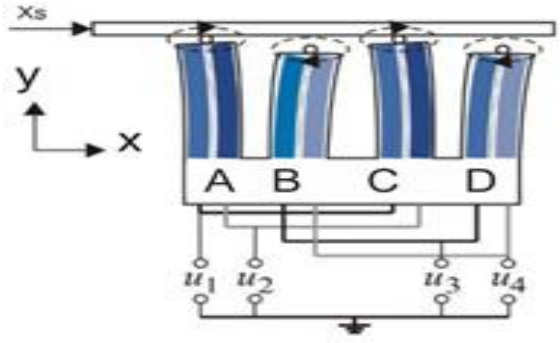

Figure 2: Nexline configuration of Piezo walk drive.

In the above figure, we can see that 4 voltages need to be applied at different piezo actuators to achieve the desired motion. Voltages 'U1' and 'U3' result in the expansion of the actuators, while voltages 'U2' and 'U4' result in the contraction, producing walk drive.

Mathematical Analysis:

It is assumed that the first pair of the legs is controlled with the driving voltages V1 and V2,

while V3 and V4 control the second pair. It is also assumed that two legs in a pair are controlled with the same voltages and that all legs have the same physical characteristics. This means that displacements of the two legs in one pair will be the same in every time instance. It is shown that displacements of the legs that form the i-th pair (i = 1, 2) in x- and y-direction are-

$$x_{p1/2}(t) = k_1 (V_{1/3}(t) - V_{2/4}(t)) \quad (3.a)$$

$$y_{p1/2}(t) = k_2 (V_{1/3}(t) + V_{2/4}(t)) \quad (3.b)$$

In (3) k1 and k2 are known constants, calculated according to (1) and (2). From (3) it can be concluded that driving voltages difference controls displacement in x-direction, while their sum controls y-direction displacement. It is now assumed that vector of the control voltages V = [V1 V2 V3 V4] T is defined as -

$$\underbrace{\begin{bmatrix} V_1(t) \\ V_2(t) \\ V_3(t) \\ V_4(t) \end{bmatrix}}_{\mathbf{V}(t)} = \underbrace{\frac{1}{2}\begin{bmatrix} 1 & 1 & 0 & 0 \\ 1 & -1 & 0 & 0 \\ 0 & 0 & 1 & 1 \\ 0 & 0 & 1 & -1 \end{bmatrix}}_{\mathbf{T}} \cdot \underbrace{\begin{bmatrix} f_{1p1}(t) \\ f_{2p1}(t) \\ f_{1p2}(t) \\ f_{2p2}(t) \end{bmatrix}}_{\mathbf{f}(t)} \Leftrightarrow \mathbf{V}(t) = \mathbf{T} \cdot \mathbf{f}(t) \quad (4)$$

where f1p1 and f2p1, f1p2 and f2p2 are time functions to be defined. Vector f will be denoted as moving vector. Matrix T defines coordinate transformation between moving vector and driving voltages. Using (4) in (3) it can be written as

$$x_{p1/2}(t) = {}^{k}1\ {}^{f}2p/2^{(t)} \quad (5.a)$$

$$y_{p1/2}(t) = k_2\ f_{1p/2}(t) \quad (5.b)$$

From (5) it is obvious that by defining vector f desired displacements in x- and y-direction can be obtained, and by doing trajectories that legs are making can be defined. In this way it is possible to define profile of the y-direction interaction force and rod's x-direction trajectory profile.

(b) PICMAWalk

PICMAWalk uses multiple layers of piezo actuators, which are configured similar to 'V8' configuration used in combustion engines in vehicles (refer Figure 2). Each 'V' comprises of a pair of piezo actuators, which alternately compress and expand, which creates a to-and-fro motion to push the ceramic runner ahead. Every 'V' is then coupled with an identical 'V' which comes in contact with the runner when the first one loses contact, and the same cycle is repeated again.

Figure 3: PICMAWalk configuration of piezo walk drive.

(c) NEXACT

This configuration is a bit different from the Nexline type in the sense that the entire piezo actuator undergoes a shear bending when experienced a voltage. Alternate pair of piezo actuators bend in the same direction (say contraction) and the other alternate pair bends in the opposite direction (expansion).

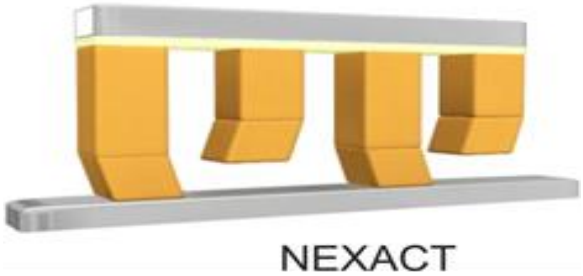

Figure 4: NEXACT configuration of piezo walk drive.

4.FEATURES

a) Very high resolution.
b) High force generation and stiffness.
c) Motors can hold a position with zero operating voltage, and leakage currents do not affect the integrity of piezo drive.
d) Piezo walk drives neither create nor are influenced by magnetic field, and can be applied for super-conductivity experiments.
e) These motors even work in vacuum and UV-light environments.

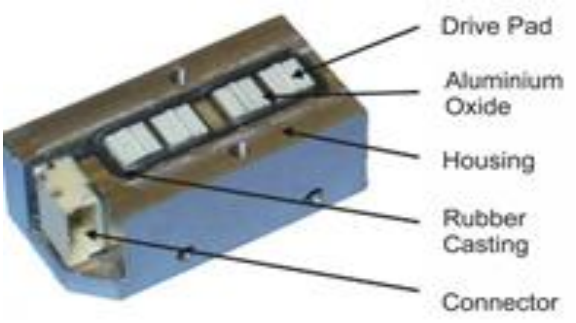

Figure 5: Physical appearance of piezo walk drive motor.

III.PIEZOELECTRIC INERTIA MOTORS

1.OVERVIEW

Piezoelectric inertia motors have originally been developed in the mid-1980s for fine positioning in microscopy applications. The fact that they have a simple construction and are controlled by a single signal, which allows for low production costs and simplifies miniaturization, inertia motors have been applied in several other fields in the last years, often in miniaturized consumer goods [4]. Thus criteria like3 the motor velocity or its power consumption and lifetime are much more important than before.

2.CLASSICAL INERTIA DRIVE MOTORS

All inertia driven motors use the inertia of a body to drive it by means of a friction contact in a series of small steps. The steps are classically assumed to consist of alternating phases of stiction and sliding, which is why inertia motors are also known as "stick-slip-drives". Figure 5 illustrates one such movement cycle of an inertia motor with a fixed stator. But due to use of static friction (sticking force) it is difficult to achieve higher speeds or smoother motions. It is previously proved that for higher speeds and smoother motions a signal of high fundamental frequency and two superposed sine waves should be used as driving signal whereas, for higher motor force more number of harmonics should be used [3].

3.RECENT DEVELOPMENTS

Researchers have proposed in theory that inertia motors can work even without phases of stiction. That is using "slip-slip" operation instead of static friction. This type of motion improves smoothness as well as the speed.

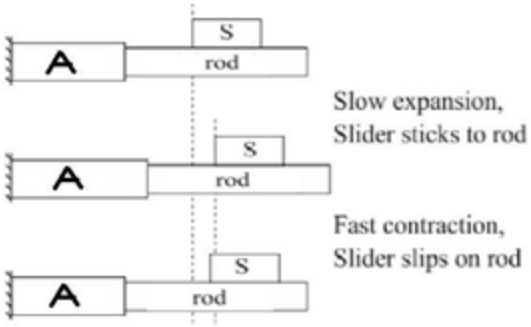

A : Actuator S: Slider

Figure 5: Classic inertia motor operation cycle.

This fact has been gaining wider recognition since only a few years. Some authors [5, 6] have described inertia motors operating in both stick–slip and slip–slip mode, but the principal advantages, disadvantages and limitations of the two modes of operation are explained in detail by [2, 3, 4]. Here, we shall discuss the experiment and compare the results of both the types.

4.THE EXPERIMENT

The aim of the experiment is to compare the velocity and the smoothness of the inertia motor in different states (discrete or continuous) and operations (stick-slip or slip-slip).

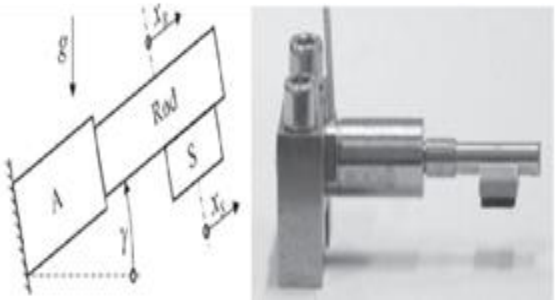

A: Actuator S: Slider

Figure 6: Slip-Slip configuration.

Figure 6 shows the model which is the basis of the following analysis. A slider of mass 'ms' hangs below the driving rod. xR(t) and xS(t) are the displacements of rod and slider, respectively. The contact force 'Fc' between rod and slider results from the gravitational force 'Fg' and an external force 'Fm', both assumed to act on the center of gravity 'C' of the slider. The friction force 'Ff(t)' acts between rod and slider. In this first part often analysis, the piezoelectric actuator that moves the rod is not considered and the displacement 'xR(t)' of the rod is

regarded as the system input which is limited by $0 \leq xR(t) \leq xR,max$.

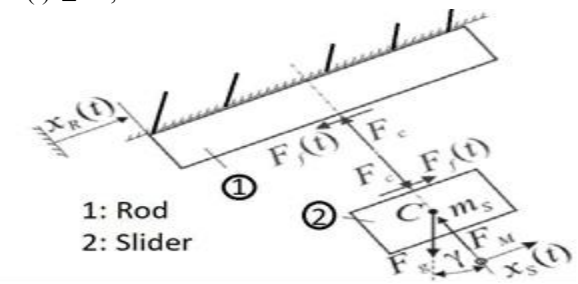

Figure 6: Rigid body model of a simple translational inertia motor.

4.1 Assumptions:

- Rod and slider are regarded as rigid bodies.
- The rod is excited purely axially, there is no lateral movement.
- Rotational effects of all forces are neglected.

4.2 Performance Indicators:

4.2.1 Steady State Velocity:

The velocity of the slider is never constant it varies over time or/and displacement. It is found that the velocity increases with every period of wave and then reaches the steady state speeds. Thus higher the frequency the quicker the steady state can achieved. This can be seen in the plot below.4.3.2 Smoothness indicator:

A smooth slider motion is always desirable. Here ,the magnitude of the inverse of the relative spread between minimum and maximum slider velocity is used as the indicator ςp for the smoothness of the slider motion in period p:

$$\varsigma_p = \frac{|{}^{v}p|}{max_p(x_s(t)) - min_p(x_s(t))} \qquad (6)$$

4.5 ANALYSIS

4.5.1 Discrete Stick-Slip operation:

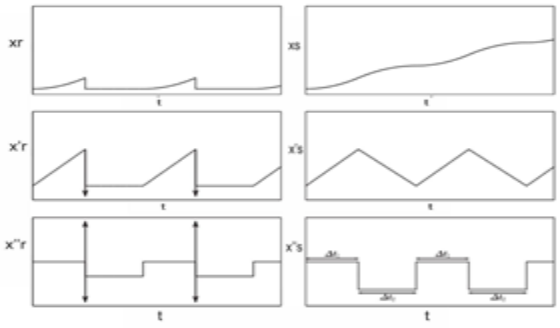

Figure 8: Displacement (x), velocity ($\dot{x}$), and acceleration ($\ddot{x}$) of rod (index R) and slider (index S) in discrete stick–slip operation. All scales of the same type (time, displacement, velocity, acceleration) are equal.

MOTION CYCLE:

a. Acceleration phase (length t1): The rod accelerates with aR = a+ 0 until it reaches its maximum position xR,max, with ≤ 1 so that the slider sticks to the rod and thus makes the same movement.
b. Pull-back (infinitely short): The rod returns to xR(t) = 0. Due to the assumption of unlimited rod velocity and acceleration, this phase is infinitely short. The (infinite) rod acceleration is larger than a+ 0 , thus the slider starts to slide.

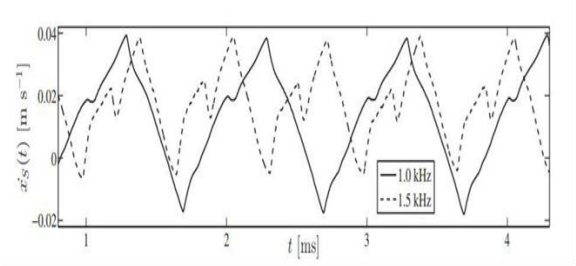

Figure 7: Steady state velocity of stator.

c. Deceleration phase (length t2): The rod is at rest, the slider is continuously decelerated by sliding friction until it also comes to rest.

4.5.2 Continuous Stick-Slip operation:

MOTION CYCLE:

a. First acceleration phase (length t1): The rod accelerates with aR = a+ 0 until it reaches its maximum position xR,max. As ≤ 1 in this stick–slip mode, the slider sticks to the rod and thus makes the same movement.
b. Pull-back (infinitely short): The rod returns to xR(t) = 0. Due to the assumption of unlimited rod velocity and acceleration, this phase is infinitely short. The (infinite) rod acceleration is larger than a+ 0 , the slider begins to slide on the rod.
c. Deceleration phase (length t2): The rod again accelerates with aR. Because the slider velocity is still higher than the rod velocity, the slider is continuously decelerated by sliding friction.

d. Acceleration phase (length t1 − t2): When (increasing) rod velocity and the (decreasing) slider velocity are equal, a new phase of stiction begins during which the slider moves with the rod and is thus accelerated with aR.

4.5.3 Discrete Slip-Slip operation:

The movement cycle is the same as that of stick-slip discrete type but the only difference is that here the acceleration of stator and rotor is not equal in magnitude.

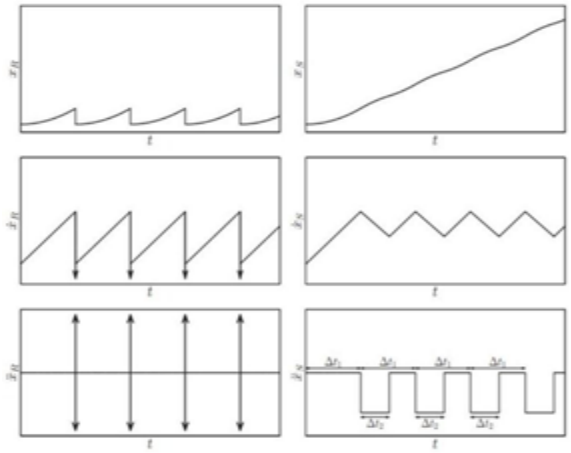

Figure 9: Displacement(x), velocity ($\dot{x}$), and acceleration ($\ddot{x}$) of rod (index R) and slider (index S)in continuous stick–slip operation. All scales of the same type (time, displacement, velocity, acceleration) are equal and as in Fig. 8.

4.5.4 Continuous Slip-Slip operation:

Other than in the other modes with periodic drive signals, in continuous slip–slip mode the mean velocity of the slider continuously increases in every period asymptotically towards a saturation value.

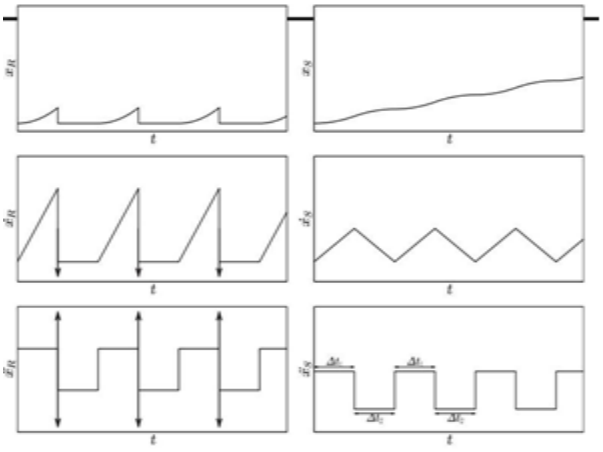

Figure 10:Displacement (x), velocity ($\dot{x}$), and acceleration ($\ddot{x}$) of rod (index R) and slider (index S) in discrete slip–slip operation with = aR/a+ 0 = 2. All scales of the same type (time, displacement, velocity, acceleration) are equal and as in Fig. 8.

Also, the time period for deceleration is considerably lower than that of acceleration.

4.6 CONCLUSIONS

The maximum motor performance achievable in these modes was investigated. One major result is that the maximum velocity reachable in stick–slip operation and with discrete steps is limited principally, while continuous slip–slip operation

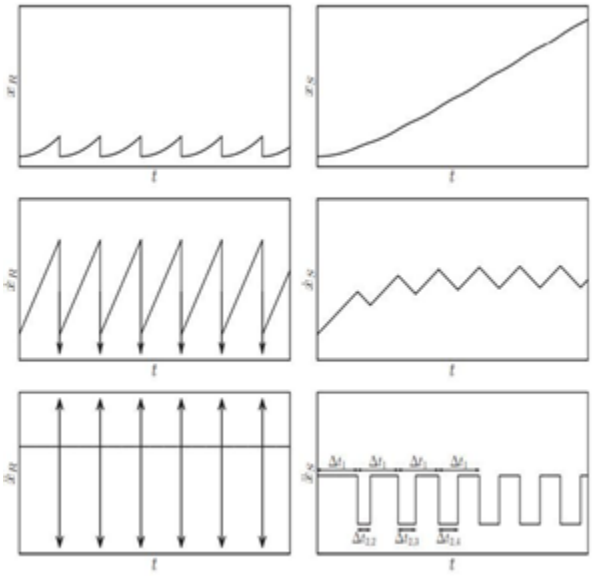

Figure 11: Displacement (x), velocity ($\dot{x}$), and acceleration ($\ddot{x}$) of rod (index R) and slider (index S) in continuous slip–slip operation with = a/a+ 0 = 2. All scales of the same type (time, displacement, velocity, acceleration) are equal and as in Fig. 8.

allows very high velocities. It was also found that, for the investigated driving signals whose frequency is proportional to the inverse of the square root of the actuator stroke, the motor velocity is proportional to the square root of the actuator stroke. The presented results show a clear advantage of slip–slip operation for the design of high velocity inertia motors. This theoretical result is supported by the fact that almost all such motors, reaching high velocities up to 300 mm s−1 and published mainly in the last few years [5, 6]. The above results are experimentally verified in [4].

IV. ULTRASONIC MICRO MOTORS

1. OVERVIEW

Piezoelectric ultrasonic micro motors are classified according to-

a. Their operation - rotary type or linear type;
b. Device geometry - rod type, ring type, disc type and cylinder types;
c. wave generation - standing wave and travelling wave.

In piezo ultrasonic motor the biggest challenge is to generate high frequency input signal. Requirement of

this high frequency input source is not economical. These motors are called ultrasonic due to the frequency of vibration greater than 20kHz.

2. STANDING WAVE PIEZOELECTRIC MOTOR

2.1 OPERATION PRINCIPLE

Standing wave type piezo ultrasonic motor is more economical due to less frequency demanding input voltage source. Standing wave type motor lacks control in circular motion due to discrete motion at low frequencies and low holding torque thus it is generally used in linear motion. Any point in standing wave have only single degree of freedom, that is vertical (according to convention). The diagram below represents the schematic representation of standing wave type ultrasonic linear motor.

Composite stator consists of a metallic plate sandwiched by two piezoelectric material. This piezoelectric layer consists of piezoelectric segments arranged in an alternate manner. Each segment is excited by two divisions of voltage source as seen in the diagram Figure 13 and 14. One unit includes two adjacent segments. The length of one unit should be λ, where λ is the wavelength of the standing wave.

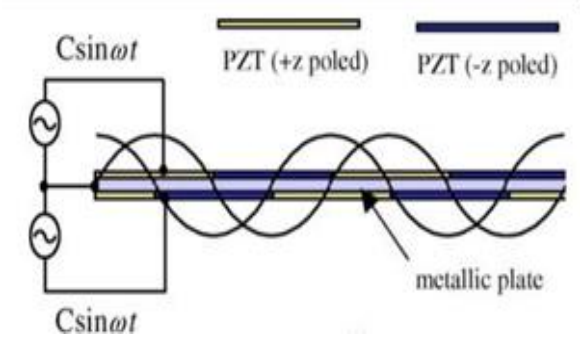

Figure 13: When the two electric signals are in-phase

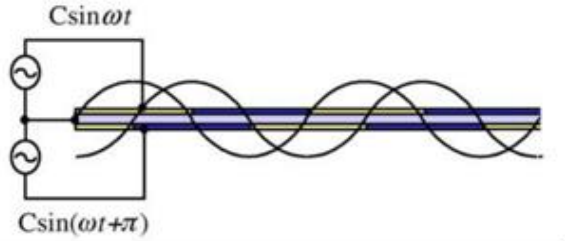

Figure 14: When the two electric signals are out-of-phase.

When two electric signals are applied to the piezoceramic plates, each plate generates its own standing wave pattern according to its polarization pattern. Figure 13 is the standing wave pattern when the two electric signals are in-phase. When there is a phase difference of π between these signals then the standing wave pattern of the lower piezoceramic plate is shifted along the stator by λ/2 in comparison to the case of being in-phase as shown in Figure 14 because one unit of piezoelectric material (2 segments) is λ. These two standing wave add up (superposition theorem) and create a new standing wave. If chosen a point on this new standing wave, it would seem to move in elliptical manner: clockwise or counterclockwise direction. If teeth, i.e. metallic extrusions, are placed at specific points on the stator, the rotor can move bi-directionally. The direction of the motion can be varied by changing the phase difference between the electric signals, either in-phase or out-of-phase.

Figure 15 shows a diagrammatic view of deformation of a point A on a tooth when the stator is applied with sinusoidal wave. Tn is the length of the tooth. The deformed point A (x0 − p, Tn + q) is displaced from the initial position by (p, q) and the corresponding deformation angle is θ. In a plate deformed in a sinusoidal form, the general expressions for the vertical deformation q and the corresponding deformation angle θ of the point A are given as Equation 7 and 8

$$q = q_0 sin(\tfrac{2\pi}{\lambda} x)_{sin}\, \omega t \,;_{x=x0} \qquad (7)$$

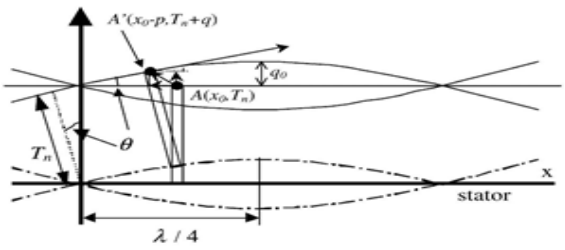

Figure 15: Deformation of a point at the tip of a tooth on the stator.

$\theta = \frac{dq}{dx}$; $x = x_0 = \frac{2\pi}{\lambda} q_0 cos(\frac{2\pi}{\lambda} x) sin\omega t$; $x = x_0$ (8)

where *q0* is the amplitude of the vertical deformation. The horizontal deformation *p* is determined from the deformation angle θ as in Eqn. 9

$p = T_n sin\theta(x)$; $x = x_0 \approx T_n \theta(x)$; $x = x_0$ for small $\theta(x)$ (9)

Accordingly, the horizontal and vertical deformations of the point *A* in Fig. 15 are determined as in Eqn. 10 and

$p_{upper} = T_n \frac{2\pi}{\lambda} q_0 cos(\frac{2\pi}{\lambda} x_0) sin\omega t$ (11.a)

$q_{upper} = q_0 sin(\frac{2\pi}{\lambda} x_0) sin\omega t$ (11.b)

Eqn. 10 and 11 denote the standing wave pattern excited by the upper piezoceramic plate. In the same manner, the deformations of the point *A* caused by the lower piezoceramic plate attached with the aforementioned spatial phase shift of $\lambda/2$ to the upper piezoceramic plate are determined as in Eqn. 12 and 13

$p_{lower} = T_n \frac{2\pi}{\lambda} q_0 cos(\frac{2\pi}{\lambda} x_0 + \frac{\pi}{2}) sin\omega t$ (12)

$q_{lower} = q_0 sin(\frac{2\pi}{\lambda} x_0 + \frac{\pi}{2}) sin\omega t$ (13)

As the upper and lower parts of the stator is bounded, the two standing waves created by the upper piezoelectric plate and the lower piezoelectric plate is coupled with each other, this give rise to a new standing wave. The final vertical deformation P and horizontal deformation Q is given by Eqn 14 and 15

$$P = T_n \frac{2\sqrt{2}\pi}{\lambda} q_0 cos(\frac{2\pi}{\lambda} x - \frac{\pi}{4}) sin\omega t \quad (14)$$

$$Q = \sqrt{2} q_0 cos(\frac{2\pi}{\lambda} x - \frac{\pi}{4}) sin\omega t \quad (15)$$

The vertical deformation *Q* of the point *A* is also the vertical deformation of the stator. The vertical deformation *Q* in Eqn 15 is zero at $x0 = ((n/2)+(3/8))\lambda$ and is its maximum at $x0 = ((n/2) + (1/8))\lambda$, where n is an integer. Because the spatial phase of *P* leads that of *Q* by $\pi/2$, the nodes and antinodes of *P* correspond to the antinodes and nodes of *Q*.

On the other hand, in addition to a spatial phase shift of $\pi/2$ between the piezoceramic plates, when the electric signal to the lower piezoceramic plate is out-of-phase, i.e. a temporal phase shift of π, with that to the upper plate, the horizontal and vertical deformations of the point *A(x0, Tn)* caused by the lower piezoceramic plate are determined as in Eqn 16 and 17.

$p'_{lower} = T_n \frac{2\pi}{\lambda} q_0 cos(\frac{2\pi}{\lambda} x_0 + \frac{\pi}{2}) sin(\omega t + \pi)$ (16)

$q'_{lower} = q_0 sin(\frac{2\pi}{\lambda} x_0 + \frac{\pi}{2}) sin(\omega t + \pi)$ (17)

Like before, superimposing the two sets of deformation, Eqn 2.iv, 11, 16 and 17, leads to another standing wave as in Eqn. 18 and 19.

$$P' = T_n \frac{2\sqrt{2}\pi}{\lambda} q_0 cos(\frac{2\pi}{\lambda} x_0 - \frac{\pi}{4}) sin\omega t \quad (18)$$

$$Q' = -\sqrt{2} q_0 cos(\frac{2\pi}{\lambda} x + \frac{\pi}{4}) sin\omega t \quad (19)$$

The vertical deformation *Q* of the point *A* is also the vertical deformation of the stator. *Q* described by Equation 19 is zero at $x0 = ((n/2) + (1/8))\lambda$ and is its maximum at $x0 = ((n/2)+(3/8))\lambda$, where *n* is an integer. Because the phase of *P* lags behind that of *Q* by $\pi/2$, the nodes and antinodes of *P* correspond to the antinodes and nodes of *Q*, respectively. The horizontal deformation *P* also has linear relationship at *x0* with the vertical deformation *Q* .

For the motor to perform identically in forward and backward direction $|P| = |-P|$. Eqn 14 and 18 we get:

$2cos(\frac{2\pi}{\lambda} x_0) cos(\frac{\pi}{4}) = 0$ (20)

The solution of Eqn 20 is $x0 = (2n + 1/4)\lambda$. This result means that if we place the teeth every $x0 = (2n + 1/4)\lambda$ of the stator (from the left end), the motor can move on the rail forward or backward, depending on the phase difference between electric driving signals, with exactly equal performance in both directions. Thus, the tooth positions correspond to every junction of two piezoceramic elements of opposite polarity in the lower ceramic plate.

Fig. 16 and Fig. 17 shows the overall deformation of the two piezoceramic plates when driven by out-of-phase sinusoidal electric signals. In this figure, the solid lines denote the vertical deformation *Q* of the stator and the white arrows denote the direction of each tooth motion when in contact with a rail. The maximum vertical deformation occurs at the right of each tooth, $\lambda/8$ away from each tooth. In addition, each tooth moves in a clockwise direction in response to the excitation. The clockwise motion of each tooth

is centered at the node of the vertical deformation *Q*, which is located on its left hand side.

When the two piezoelectric plates are driven with in phase voltage input, the nodes and antinodes of the stator deformation are exchanged with each other.

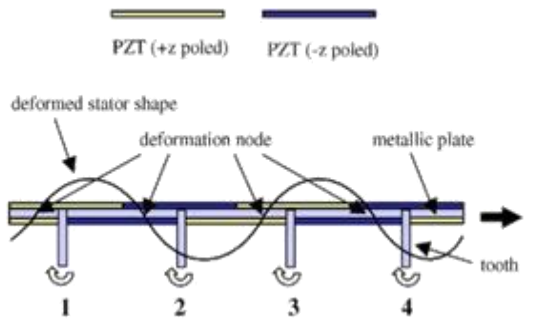

Figure 16: Forward motion by out-of-phase driving.

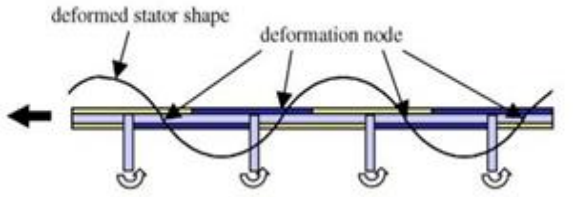

Figure 17: Backward motion by in-phase driving.

Additionally, the maximum deformation occurs at the left of each tooth, *λ/8* away from each tooth as shown in Figure 16. Therefore, the linear motor can move back and forth according to a phase difference of either 0 or π between the input voltage signal applied to the two piezoceramic plates.

When the two piezoelectric plates are driven with in phase voltage input, the nodes and antinodes of the stator deformation are exchanged with each other.

3. TRAVELLING WAVE PIEZO ULTRASONIC MOTOR

3.1 OPERATION PRINCIPLE

Rotary motion can be achieved by applying a travelling wave to the piezoelectric ultrasonic micro motor. By superimposing two standing waves of having space-time phase difference of 90 degree, a travelling wave can be generated. The travelling wave combines two standing waves with a 90 degree phase difference both in time and in space. Due to the coupling of longitudinal and transverse waves an elliptical locus is drawn by surface particle of the elastic body. Thus travelling wave type ultrasonic motor needs a dual power supply.

A hollow ring type travelling piezoelectric motor is shown in figure 18

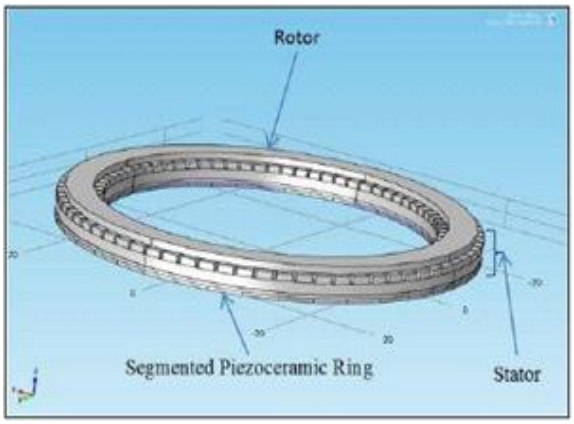

Fig 18: Hollow ring type Piezoelectric ultrasonic motor depicting stator and the rotor. Designed in COMSOL Multiphysics 5.3 tool

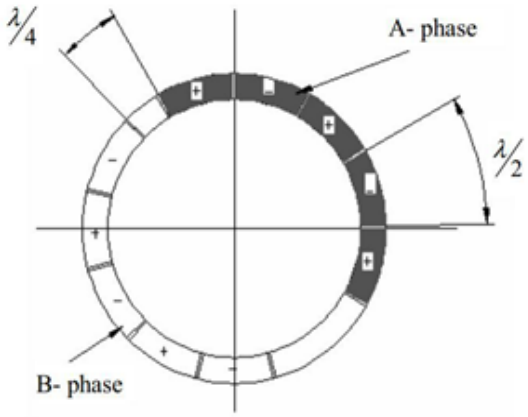

Fig 19: Piezoelectric disc and electrode arrangement of the USM

Polarization area can be divided into three parts: A-phase, B-phase and single-electrode.

A-phase electrode provides $cos(k\theta)$ vibration, and B-phase electrode provides $sin(k\theta)$ vibration. A traveling-wave is produced by driving these two modes with 90° temporal phase shifting. A-phase and B-phase provides standing wave individually. The superposition of these standing waves produce a traveling-wave used in traveling-wave type USM Positive (+) and negative (-) signs show the polarized directions. When a positive voltage is applied to a segment indicated by (+), piezoelectric ceramic will expand. With a negative voltage it will contract. The reverse occurs for a segment (-)

Displacement caused by A-phase is:

$$y1 = Asin(\omega t).sin(\omega\theta) \quad (21)$$

Displacement caused by B-phase is:

$$y2 = A\cos(\omega t).\cos(\omega\theta) \quad (22)$$

Where A , θ, ω and t are vibration amplitude, phase angle, vibration frequency and vibration time respectively. n = $\omega/v = 2\pi/\lambda$ is wave number on the circumference of the stator, λ is wavelength. So the superposed displacement is:

$$y = y1 + y2$$
$$= A\sin(\omega t).\sin(n\theta) + A\cos(\omega t).\cos n\theta$$
$$= A\cos(n\theta - \omega t) \quad (23)$$

The above equation shows a flexible travelling wave which will be generated through the stator.

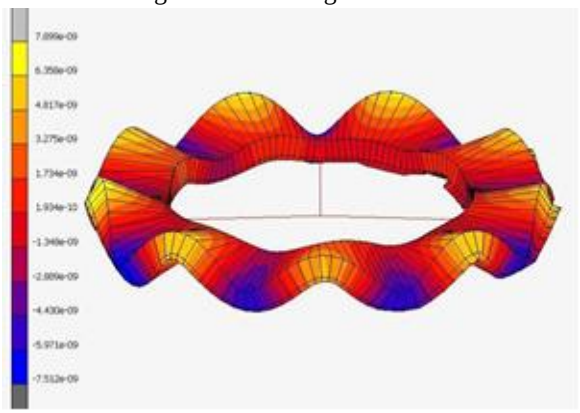

Fig 20: 9th mode bending state of stator in Travelling wave USM(Yellow color denotes maximum positive vertical displacement and blue color denotes maximum negative vertical displacement). Simulation done in MSC Marc and Mentat tool.

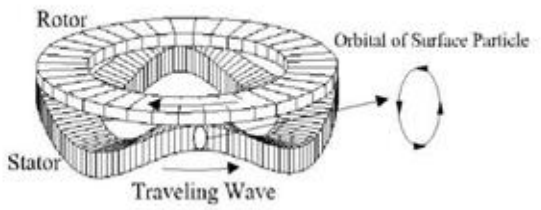

Fig 21: Shows the rotor motion is in opposite direction of the motion of the travelling wave generated by stator, due to application of friction in negative direction as compared to the motion of the stator. If considered a point on stator it moves in an elliptical manner. Image courtesy [17]

V CONCLUSION

Piezo actuators and motors have attracted immense research owing to the versatility, advantages, small size and low power consumption. These actuators find varied applications in the domain of micro robotics, medical science, computer industry etc.

REFERENCES

[1] Development of a new standing wave type ultrasonic linear motor: Yongrae Roh, Jaehwa Kwon, School of Mechanical Engineering, Kyungpook National University, Sankyukdong 1370, Bukgu, Daegu 702-701, South Korea Department of Sensor Engineering, Kyungpook National University, Sankyukdong 1370, Bukgu, Daegu 702-701, South Korea, 7 January 2004. *spiedigitallibrary*

[2] K. Matsusaka, S. Ozawa, R. Yoshida, T. Yuasa, Y. Souma, Ultracompact optical zoom lens for mobile phone, in: Proceedings of SPIE-IS&T Electronic Imaging, vol. 6502 (2007) p. 650203 (10 pp.). *conference proceeding*

[3] Springer publication: Hunstig, M., Hemsel, T., Sextro, W.: Stick-slip and slip-slip operation of piezoelectric inertia drives. Part I: ideal excitation. Sens. Actuators A 200, 90–100 (2013).

[4] Springer publication Hunstig, M., Hemsel, T., Sextro, W.: Stick-slip and slip-slip operation of piezoelectric inertia drives—Part II: frequency limited excitation. Sens. Actuators A 200, 79–89 (2013).

[5] Springer publication: Hunstig, M., Hemsel, T., Sextro, W.: High-velocity operation of piezoelectric inertia motors: experimental validation.

[6] Y. Okamoto, R. Yoshida, Development of linear actuators using piezoelectric elements, Electronics and Communications in Japan, Part 3 81 (1998) 11–17. Translated from Denshi Joho Tsushin Gakkai Ronbushi, vol. J80-A, No. 10, October 1997, 1751–1756.

[7] NCBI publication: J. Lee, W.S. Kwon, K. Kim, S. Kim, A novel smooth impact drive mechanism actuation method with dual-slider for a compact zoom lens system, Review of Scientific Instruments 82 (2011) 085105.

[8] Piezo motors/positioners: http://www.piezo-motor.net/pdf/PI_Brochure_Piezomotor_Piezo_ Motor_PiezoWalk_Ultrasonic_Actuato r.pdf

[9] IEEE transaction: Piezoelectric Ultrasonic Motor, R. Inaba, A. Tokushima, O. Kawasaki, Y. Ise and H. Yoneno Central Research Laboratory, Matsushita Electrical Industrial Co. Osaka, Japan.

[10] Survey of the various operating principles of Ultrasonic Piezo Motors, by K Spanner, Physik instrumente GmbH. &Co. KG, Karlsruhe, Germany, White paper for ACTUATOR 2006.

[11] Piezo motion control tutorialhttp://www.pi-usa.us/piezo_motion_tutorial/

[12] Piezo walk motors https://www.physikinstrumente.com/en/technology/pi ezoelectric-drives/piezowalk-piezo-motors/

[13] Design and Simulation of a Piezoelectric Ultrasonic Micro Motor , Parul Parag Patel, Dr Premila Manohar, M S Ramaiah Institute of Technology, Bangalore, India.

[14] A ring-type traveling wave ultrasonic motor using optimized design of piezoelectric ceramics, Xiaoxiao Dong, Minqiang Hu, Long Jin, Peng Pan College of Electrical Engineering, Southeast University, China.

[15] THEORETICAL ANALYSIS AND DESIGN OF ULTRASONIC MICROMOTORS, Cui Tainhoiig , Wa71g Lidiiig Lu Qioiigyiiig and To7ig Xiaodoirg, Changchun Institute of Optics and Fine Mechanics, Chinese Academy of Sciences Changchun, Jilin 130022 P. R. China

[16] Analysis and Design of a Ring-type Traveling Wave Ultrasonic Motor, Ming Hao and Weishan Chen, Department of mechatronic Engineering Harbin, Institute of Technology Harbin, Heilongjiang province, P.R. China

[17] Rotary Ultrasonic Motors Actuated By Traveling Flexural Waves, Shyh-Shiuh Lih, Yoseph Bar-Cohen, Jet Propulsion Laboratory, California Institute of Technology, Pasadena, CA 91109 and Willem Grandia, Quality Material Inspection (QMI), Costa Mesa, CA 92627.

[18] FPGA Based Control of a Walking Piezo Motor Tarik Uzunovic, Edin Golubovic, Asif Sabanovic Mechatronics Program Sabanci University Istanbul, Turkey.

[19] Springer publication: Micro Piezoelectric ultrasonic motors, K Uchino, S Catagay, B. Koc, S. Dong, P. Bouchilloux, M. Strauss, Journal of Electroceramics, July 2004

[20] Using a Walking Piezo Actuator to Drive and Control a High-Precision Stage Roel J. E. Merry, Student Member, IEEE, Niels C. T. de Kleijn, Marinus J. G. van de Molengraft, and Maarten Steinbuch, Senior Member, IEEE.

[21] Springer publication: FEM Analysis and parameter optimization of linear piezoelectric motor Macro Driven, Z. Tiemin, C. Fei, L. Shenghua, W. Sheng.

[22] Springer publication: Friction Experiment Study on the Standing Wave Linear Piezoelectric Motor Macro Driven, L. Liang, T. Zhang, P. Huang, D. Kong.

[23] Springer publication: Ultrasonic motor - Technologies and applications, C. Zhao.

[24] Pyroelectricity versus conductivity in soft lead zirconate titanate (PZT) ceramics, Talal M. Kamel and G. de Witha, Laboratory of Materials and Interface Chemistry, Eindhoven University of Technology, 5600 MB Eindhoven, The Netherlands (Received 4 May 2007; accepted 29 August 2007) Cambridge Core Journals.